Inner- and Outer-Sphere Pathways in the Reaction between (Pyrazine)pentaammineruthenium(III) and (Ethylenediaminetetraacetato)cobaltate(II): Direct Proof That the Successor Binuclear Complex Represents a Dead End[1a]

Grant C. Seaman[1b] and Albert Haim*

Contribution from the Department of Chemistry, State University of New York, Stony Brook, New York 11794. *Received July 22, 1983*

Abstract: The reaction between $[Ru(NH_3)_5(pz)]^{3+}$ (pz = pyrazine) and $[Co(EDTA)]^{2-}$ ($EDTA^{4-}$ = ethylenediaminetetraacetate) proceeds via parallel outer-sphere and inner-sphere pathways. The outer-sphere pathway yields $[Ru(NH_3)_5(pz)]^{2+}$ and $[Co(EDTA)]^-$ directly with a rate constant of 1.0×10^3 M^{-1} s^{-1} at 25 °C and ionic strength 0.10 M. The inner-sphere pathway produces the dead-end binuclear intermediate $[(NH_3)_5Ru^{II}(pz)Co^{III}(EDTA)]^+$ with a rate constant of 2.5×10^3 M^{-1} s^{-1} at 25 °C and ionic strength 0.10 M. The intermediate disappears by intramolecular electron transfer (rate constant of 16.9 s^{-1} at 25 °C and ionic strength 0.10 M) followed by dissociation to produce $[Ru(NH_3)_5(pz)]^{3+}$ and $[Co(EDTA)]^{2-}$, which in turn react by the outer-sphere pathway described above. The rate constant for the outer-sphere reaction between $[Ru(NH_3)_5(pz)]^{2+}$ and $[Co(EDTA)]^-$ has been measured as 3.2 M^{-1} s^{-1} at 25 °C and ionic strength 0.10 M. A detailed mechanistic discussion of the title reaction is presented, and comparisons are made with the analogous reactions where pyrazine is replaced by 4,4′-bipyridine or the cobalt center is replaced by ruthenium.

The detection of binuclear complexes represents a key observation in the elucidation of the mechanisms of oxidation reduction reactions between transition-metal complexes.[2] Often, the binuclear complexes, whether precursor[3] or successor,[4] are transient intermediates along the pathways that connect reactants to products. However, in some instances, e.g., the $[Fe(CN)_6]^{3-}$–$[Co(EDTA)]^{2-}$ system,[5] the binuclear complex detected as the major product immediately after mixing the reactants[6,7] represents a dead end. In other words, the binuclear species is not generated as an intermediate along the pathway that leads from mononuclear reactants to mononuclear products but is formed in an unproductive side reaction. In previous work,[8] we sought to characterize the binuclear complex that was anticipated to be produced as a dead-end intermediate in the reaction between $[Ru(NH_3)_5(bpy)]^{3+}$ (bpy = 4,4′-bipyridine) and $[Co(EDTA)]^{2-}$ ($EDTA^{4-}$ = ethylenediaminetetraacetate). To our surprise,[8] that reaction was found to proceed exclusively (>95%) by an outer-sphere mechanism, and, of course, no binuclear complex could be characterized. In contrast, we have found that the reaction between $[Ru(NH_3)_5(pz)]^{3+}$ (pz = pyrazine) and $[Co(EDTA)]^{2-}$ results in high initial yields of the binuclear intermediate I, and we report herein our

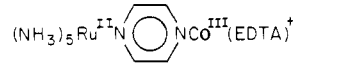

I

detailed kinetic studies of the forward and reverse reactions in the $[Ru(NH_3)_5(pz)]^{3+/2+}$–$[Co(EDTA)]^{-/2-}$ system.

Experimental Section

Materials. $[Ru(NH_3)_5(pz)H]Br_4$ was prepared from $Ru(NH_3)_5Cl_3$ as described previously.[9] The purity of the product was ascertained spectroscopically after reduction with ascorbic acid at pH 5. The observed maximum at 474 nm with a molar absorbance of 13 500 M^{-1} cm^{-1} is in excellent agreement with the previously reported values 472 nm and 13 300 M^{-1} cm^{-1} for $[Ru(NH_3)_5(pz)]^{2+}$.[10] A stock solution of cobalt(II) chloride was prepared by dissolution of the reagent grade material in purified water. The concentration of cobalt in the solution was determined spectrophotometrically as the pyridinedicarboxylate complex.[11] Solutions of $[Co(EDTA)]^{2-}$ were prepared when needed by adding a 10% excess of Na_2H_2EDTA to the cobalt(II) solution. Reagent grade lithium perchlorate was recrystallized from water. The sample of K[Co(EDTA)] was from our previous work.[5] The water used in all experiments was purified as described previously.[8] All other chemicals were of reagent grade and used as received.

Kinetic Measurements. The reaction between $[Ru(NH_3)_5(pz)]^{3+}$ and $[Co(EDTA)]^{2-}$ was studied in a Durrum-110 stopped-flow apparatus. Absorbance vs. time data, displayed in an Omnigraphic 2000 recorder connected to a Nicolet Explorer III A oscilloscope, were digitized with a Hewlett-Packard 9864A digitizer and then processed in a Hewlett-Packard 9820 calculator. Values of k_{obsd}, observed first-order rate constants, were calculated from a least-squares fitting of the equation $\ln (A_t - A_\infty) = \ln (A_0 - A_\infty) - k_{obsd}t$, where A_t, A_∞, and A_0 are absorbances at time t, 0 (first point), and long times (8–10 half lives), respectively. The reaction between $[Ru(NH_3)_5(pz)]^{2+}$ and $[Co(EDTA)]^-$ was studied in a Cary 17 spectrophotometer and the absorbance vs. time data were treated as outlined above in order to obtain values of k_{obsd}.

Results

Stoichiometry. When solutions of $[Ru(NH_3)_5(pz)]^{3+}$ (10^{-5} M) and $[Co(EDTA)]^{2-}$ (10^{-3} M) are mixed at room temperature, a purple color develops immediately and then fades, within a few seconds, to the yellow color characteristic of $[Ru(NH_3)_5(pz)]^{2+}$. Spectrophotometric examination of the product solution in the 600–400-nm range showed no additional absorbance changes for at least several minutes. The stoichiometry of the overall reaction (reactants to yellow product) is described by eq 1. With $[Ru(NH_3)_5(pz)]^{3+}$ (1.03×10^{-5} M) and $[Co(EDTA)]^{2-}$ (7.26×10^{-3} M), the forward reaction in eq 1 proceeds quantitatively as seen

$$[Ru(NH_3)_5(pz)]^{3+} + [Co(EDTA)]^{2-} \rightleftharpoons [Ru(NH_3)_5(pz)]^{2+} + [Co(EDTA)]^- \quad (1)$$

(1) (a) This work was supported by Grant CHE-8203887 from the National Science Foundation. (b) Abstracted in part from the B.S. Thesis of G.C.S., State University of New York at Stony Brook, May 1981.
(2) Haim, A. Prog. *Inorg. Chem.* **1983**, *30*, 273.
(3) Gaswick, D. G.; Haim, A. *J. Am. Chem. Soc.* **1974**, *96*, 7845.
(4) Melvin, W. S.; Haim, A. *Inorg. Chem.* **1977**, *16*, 2016.
(5) Rosenheim, L.; Speiser, D.; Haim, A. *Inorg. Chem.* **1974**, *13*, 1571.
(6) Adamson, A. W.; Gonick, E. *Inorg. Chem.* **1963**, *2*, 129.
(7) Huchital, D. H.; Wilkins, R. G. *Inorg. Chem.* **1967**, *6*, 1022.
(8) Phillips, J.; Haim, A. *Inorg. Chem.* **1980**, *19*, 76.
(9) Yeh, A.; Haim, A.; Tanner, M.; Ludi, A. *Inorg. Chim. Acta* **1979**, *33*, 51.
(10) Creutz, C.; Taube, H. *J. Am. Chem. Soc.* **1973**, *95*, 1086.
(11) Hartkamp, H. Z. *Anal. Chem.* **1961**, 251.

0002-7863/84/1506-1319$01.50/0

Table I. Kinetics of the Reaction between $Ru(NH_3)_5pz^{3+}$ and $CoEDTA^{2-}$ at 25.0 °C, pH 4.40 ± 0.05, Ionic Strength 0.10 M[a]

$[CoEDTA^{2-}]$, $M \times 10^4$	k_{obsd}^{474}, s^{-1}	k_{obsd}^{530}, s^{-1}	k_{obsd}^{iso}, s^{-1}	isosbestic wavelength, nm
3.06	0.222			
6.12	0.451, 0.424		17.7	532
12.2	0.713, 0.730	0.867, 0.889	20.7, 21.9	518
24.5	1.07, 1.03	1.18, 1.41	23.4, 26.7	509
24.5	1.05, 1.00	1.21	26.6	509
24.5[b]	1.05, 1.09	1.61, 1.28	24.4, 25.4	509
24.5[c]	1.06, 1.11	1.57, 1.31	27.5, 27.1	509
24.5[d]	1.04	1.27	25.6	509
36.7	1.21, 1.30	1.51, 1.49	29.4, 30.2	505
36.7	1.33	1.37		
48.4	1.28, 1.47	1.48, 1.63	34.8, 32.7	504
48.4	1.53	1.66	35.6	504
62.9	1.46, 1.53	1.70, 1.85	39.2, 40.6	502
62.9	1.53	1.76		
72.6	1.63, 1.48	1.83, 1.96	42.0, 40.9	501

[a] With $[Ru(NH_3)_5(pz)^{3+}] = (0.9\text{–}1.1) \times 10^{-5}$ M. Each entry is the average of four replicate measurements with the same pair of solutions. [b] $[Ru(NH_3)_5(pz)^{3+}] = 2.41 \times 10^{-6}$ and 2.58×10^{-6} M for the first and second entry, respectively. [c] $[Ru(NH_3)_5(pz)^{3+}] = 4.91 \times 10^{-6}$ and 7.43×10^{-6} M for the first and second entry, respectively. [d] $[Ru(NH_3)_5(pz)^{3+}] = 1.05 \times 10^{-5}$ M.

by comparing the calculated absorbances at 474 (maximum for $[Ru(NH_3)_5(pz)]^{2+}$ with molar absorbance 1.35×10^4 M^{-1} cm^{-1}; molar absorbance of $[Co(EDTA)]^-$ 81 M^{-1} cm^{-1}) and 538 nm (maximum for $[Co(EDTA)]^-$ with molar absorbance 301 M^{-1} cm^{-1}; molar absorbance of $[Ru(NH_3)_5(pz)]^{2+}$ 2.09×10^3 M^{-1} cm^{-1}) with the observed values. The comparison, observed absorbances (range in instrument 0.2–1-cm cell) 0.690 and 0.125 at 472 and 538 nm, respectively, vs. calculated values, 0.695 and 0.123, shows that the reaction proceeds to completion (>99%) as expected from the equilibrium constant $K_2 = 343$ calculated from the $E°$ values at 25 °C and ionic strength 0.2 M[12] or 0.1 M[13] for the $[Ru(NH_3)_5(pz)]^{3+/2+}$ (0.52 V) and $[Co(EDTA)]^{-/2-}$ (0.37 V[14]) couples.

Kinetics. Mixing of $[Ru(NH_3)_5(pz)]^{3+}$ with $[Co(EDTA)]^{2-}$ in the stopped-flow apparatus clearly showed that the overall reaction represented by eq 1 proceeds in two stages. Observations were made at three wavelengths: 474 nm (the maximum for $[Ru(NH_3)_5(pz)]^{2+}$, 530 nm (the predicted maximum for I; see below), and an intermediate wavelength. At 474 nm the absorbance increases in a biphasic mode. For example, with $[Co(EDTA)]^{2-}$ (7.26×10^{-3} M), there is a rapid absorbance increase that is complete in about 0.1 s and is followed by a slower increase that ends in about 2 s. Under the same conditions, at 530 nm the absorbance first increases rapidly (~0.1 s) and then decreases slowly (~2 s). The time at which the absorbance reaches a maximum and the magnitude of the absorbance at that time vary with changing $[Co(EDTA)]^{2-}$ concentration. The maximum absorbance increases with increasing $[Co(EDTA)]^{2-}$ concentration whereas the maximum time decreases with increasing concentration. At an intermediate wavelength, a single exponential increase in absorbance with the characteristic time of the rapid phase is observed. The wavelength at which only a monophasic reaction is observed decreases with increasing $[Co(EDTA)]^{2-}$ concentration.

Rate constants for the slow phase were measured at 474 and 530 nm. Good first-order plots (~3 half-lives, correlation coefficient 0.999) were obtained at both wavelengths as long as the initial absorbances were taken after 8–10 half lives of the fast phase had elapsed. Values of k_{obsd}^{474} and k_{obsd}^{530} for the measurements at 474 and 530 nm are listed in columns 2 and 3 of Table I. It will be seen that the values of k_{obsd}^{474} or k_{obsd}^{530} are independent of the $[Ru(NH_3)_5(pz)]^{3+}$ concentration and depend upon the concentration of $[Co(EDTA)]^{2-}$ according to eq 2.

$$k_{obsd}^{474} \text{ or } k_{obsd}^{530} = \frac{a[(Co(EDTA))^{2-}]}{1 + b[(Co(EDTA))^{2-}]} \quad (2)$$

Nonlinear least-squares calculations yielded values of a and b (25 °C, ionic strength 0.10 M) equal to $(8.8 \pm 0.3) \times 10^2$ M^{-1} s^{-1} and 423 ± 35 M^{-1} at 474 nm and $(1.09 \pm 0.05) \times 10^3$ M^{-1} s^{-1} and 457 ± 58 M^{-1} at 530 nm.

The wavelengths at which only the rapid, monophasic absorbance changes occurred (herein after named isosbestic wavelength) were determined experimentally at each $[Co(EDTA)]^{2-}$ concentration. Measurements were made near the anticipated wavelength. At wavelengths longer than the isosbestic, the absorbance was clearly seen to reach a maximum and then to decrease. At wavelengths shorter than the isosbestic, a biphasic absorbance increase was easily discerned. In this manner, the isosbestic wavelengths were determined within 1 nm. Plots of $\ln (A_t - A_\infty)$ vs. time at these wavelengths were linear for at least 3 half-lives, and the derived values of k_{obsd}^{iso} and the corresponding isosbestic wavelengths are listed in columns 4 and 5, respectively, of Table I. k_{obsd}^{iso} varies with the concentration of $[Co(EDTA)]^{2-}$ according to eq 3, where (least-squares calculation) $c = 16.9 \pm 0.6$ s^{-1} and

$$k_{obsd}^{iso} = c + d[(Co(EDTA))^{2-}] \quad (3)$$

$d = (3.53 \pm 0.14) \times 10^3$ M^{-1} s^{-1} at 25 °C and ionic strength 0.10 M.

With ordinary concentrations of $[Ru(NH_3)_5(pz)]^{2+}$ and $[Co(EDTA)]^-$ the reverse reaction in eq 1 does not proceed to completion. Therefore, the reaction was studied in the presence of excess ascorbic acid. The latter is known to react slowly[5] with $[Co(EDTA)]^-$ and rapidly[13] with $[Ru(NH_3)_5(pz)]^{3+}$. Therefore, as rapidly as $[Ru(NH_3)_5(pz)]^{3+}$ and $[Co(EDTA)]^{2-}$ are formed by reaction between $[Ru(NH_3)_5(pz)]^{2+}$ and $[Co(EDTA)]^-$, the $[Ru(NH_3)_5(pz)]^{3+}$ is reduced back to $[Ru(NH_3)_5(pz)]^{2+}$ by the ascorbic acid. Under these circumstances, the system under study consists of the $[Ru(NH_3)_5(pz)]^{2+}$-catalyzed reduction of $[Co(EDTA)]^-$ by ascorbic acid, the rate-determining step being the reverse of eq 1. The disappearance of $[Co(EDTA)]^-$ was monitored at 384 nm, a maximum for $[Co(EDTA)]^-$ with molar absorbance 235 M^{-1} cm^{-1}, and a near minimum for $[Ru(NH_3)_5(pz)]^{2+}$ with molar absorbance ~800 M^{-1} cm^{-1}. Plots of $\ln (A_t - A_\infty)$ vs. time were linear for at least 3 half-lives, and the corresponding values of k_{obsd}^{384}, listed in column 2 of Table II, were found to vary with the concentration of $[Ru(NH_3)_5(pz)]^{2+}$ according to eq 4, where $e = (3.5 \pm 2.0) \times 10^{-5}$ s^{-1} and $f = 3.20 \pm 0.04$ M^{-1} s^{-1} at 25 °C and ionic strength 0.10 M.

$$k_{obsd}^{384} = e + f[(Ru(NH_3)_5(pz))^{2+}] \quad (4)$$

Table II. Kinetics of the Reaction between $[Ru(NH_3)_5(pz)]^{2+}$ and $[Co(EDTA)]^-$ at 25.0 °C, pH 4.40 ± 0.05, Ionic Strength 0.10 M[a]

$[Ru(NH_3)_5pz^{2+}]$, $M \times 10^5$	k_{obsd}^{384}, s^{-1}
9.93, 9.83	3.19, 3.13
19.7, 19.9	6.72, 7.05
40.0, 38.9	13.3, 13.2
79.1, 79.2	25.2, 25.8

[a] With $[CoEDTA^-] = 1.7 \times 10^{-3}$ M and [ascorbic acid] = 1.8×10^{-3} M.

Scheme I

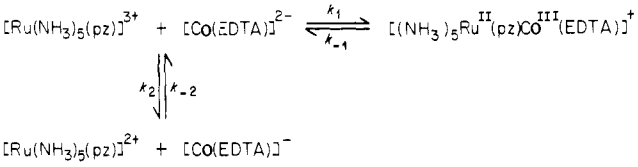

(12) Creutz, C.; Kroger, P.; Matsubara, T.; Netzel, T. L.; Sutin, N. *J. Am. Chem. Soc.* **1979**, *101*, 5442.
(13) Yeh, A. Ph.D. Thesis, State University of New York at Stony Brook, 1978.
(14) Tanaka, N.; Ogino, H. *Bull. Chem. Soc. Jpn.* **1965**, *38*, 1054.

Discussion

The bulk of the observations are consistent with mechanistic Scheme I. According to this scheme, the reaction between $[Ru(NH_3)_5(pz)]^{3+}$ and $[Co(EDTA)]^{2-}$ is viewed as proceeding via parallel outer- and inner-sphere pathways. The outer-sphere pathway k_2 produces directly the final products $[Ru(NH_3)_5(pz)]^{2+}$ and $[Co(EDTA)]^-$ and accounts for the observed rapid increase in absorbance at 474 nm. The inner-sphere pathway k_1 (also rapid) yields the binuclear complex I. The slow absorbance increase at 474 nm is then accounted for on the basis of back electron transfer in I (k_{-1} path) followed by the outer-sphere reaction k_2. The rapid absorbance increase at 530 nm followed by a slower absorbance decrease is also accounted for on the basis of Scheme I. By analogy with the similar binuclear complexes $[(NH_3)_5Ru^{II}(pz)Co^{III}(CN)_5]$ (maximum at 524 nm, molar absorbance 1.86×10^4 M^{-1} cm^{-1}),[9] $[(NH_3)_5Ru^{II}(pz)Ru^{III}(EDTA)]^+$ (maximum at 520 nm, molar absorbance 1.72×10^4 M^{-1} cm^{-1}),[12] $[(NH_3)_5Ru^{II}(pz)Rh^{III}(NH_3)_5]^{5+}$ (maximum at 528 nm, molar absorbance 1.8×10^4 M^{-1} cm^{-1}),[10] and $[(NH_3)_5Ru^{II}(pz)Rh^{III}(EDTA)]^+$ (maximum at 529 nm, molar absorbance 1.9×10^4 M^{-1} cm^{-1}),[12] the binuclear complex $[(NH_3)_5Ru^{II}(pz)Co^{III}(EDTA)]^+$ is expected to have an absorption maximum near 530 nm with molar absorbance ca. 2×10^4 M^{-1} cm^{-1}.[15] Since $[Ru(NH_3)_5(pz)]^{3+}$ does not absorb at 530 nm and $[Ru(NH_3)_5(pz)]^{2+}$ and $[Co(EDTA)]^-$ have relatively small molar absorbances at this wavelength (3.0×10^3 and 2.9×10^2 M^{-1} cm^{-1}, respectively), the rapid formation of I via pathway k_1 is accompanied by a rapid increase in absorbance. The subsequent disappearance of I via the sequence k_{-1} followed by k_2 accounts for the slow absorbance decrease. The increase in the maximum absorbance at 530 nm with increasing $[Co(EDTA)]^{2-}$ concentration is also accounted for by Scheme I. Since the disappearance of I is relatively slow compared to its formation, when the maximum absorbance is reached, I is in near equilibrium with $[Ru(NH_3)_5(pz)]^{3+}$ and $[Co(EDTA)]^{2-}$, and thus the concentration of I increases with increasing concentration of $[Co(EDTA)]^{2-}$. Finally, the occurrence of an isosbestic wavelength that decreases with increasing $[(Co(EDTA))^{2-}]$ is nicely accounted for on the basis of Scheme I. At the end of the rapid phase, near equilibrium between the reactants and I has been achieved. The slow phase corresponds to the disappearance of an equilibrium mixture of $[Ru(NH_3)_5(pz)]^{3+}$, $[Co(EDTA)]^{2-}$, and $[(NH_3)_5Ru^{II}(pz)Co^{III}(EDTA)]^+$ and the appearance of $[Ru(NH_3)_5(pz)]^{2+}$. The effective molar absorbance of the equilibrium mixture, a_{eff}, is given by eq 5 where

$$a_{eff} = \frac{a_B[I]}{[I] + [[Ru(NH_3)_5(pz)]^{3+}]} \quad (5)$$

a_B is the molar absorbance of the binuclear complex, and the absorbances of $[Ru(NH_3)_5(pz)]^{3+}$ and $[Co(EDTA)]^{2-}$ are neglected. When equilibrium between the reactants and I obtains, eq 5 becomes $a_{eff} = a_B[[Co(EDTA)]^-]K_1/(1 + K_1[[Co(EDTA)]^{2-}])$, where $K_1 = k_1/k_{-1}$. At a wavelength where the value of a_{eff} is equal to the molar absorbance of $[Ru(NH_3)_5(pz)]^{2+}$, then the transformation of the equilibrium mixture into $[Ru(NH_3)_5(pz)]^{2+}$ proceeds without an absorbance change, i.e., an isosbestic wavelength, dependent upon $[(Co(EDTA))^{2-}]$, obtains.

Although Scheme I accounts nicely for most of our general observations, there are some problems with the detailed interpretation of some of the data. However, before analyzing our data on the basis of Scheme I, it is important to determine the relationship between the measured constants k_{obsd}^{474}, k_{obsd}^{530}, and k_{obsd}^{iso} and the rate constants k_1, k_{-1}, k_2, and k_{-2}. This was accomplished by performing the following kinetic modeling. Scheme I was integrated by using the Runge–Kutta approximation,[16] and the concentrations of all species were calculated as a function of time. Input parameters, chosen to be near the values estimated from the experimental measurements, were $k_1 = 3 \times 10^3$ M^{-1} s^{-1}, $k_{-1} = 15$ s^{-1}, $k_2 = 1 \times 10^3$ M^{-1} s^{-1}, $k_{-2} = 3$ s^{-1}, $[[Ru(NH_3)_5(pz)]^{3+}]_0 = 1 \times 10^{-5}$ M and $[[Co(EDTA)]^{2-}] = (1-7) \times 10^{-3}$ M. For each concentration of $[Co(EDTA)]^{2-}$, values of A_{474}, A_{530}, and A_{iso}, the absorbance of the system at 474 and 530 nm and the isosbestic wavelength, were computed as a function of time (molar absorbances of $[Ru(NH_3)_5(pz)]^{2+}$ and I were taken as 1.4×10^4 and 5.0×10^3 at 474 nm and 3.0×10^3 and 2.0×10^4 at 530 nm). Values of k_{obsd}^{474}, k_{obsd}^{530}, and k_{obsd}^{iso} were obtained by fitting the absorbances to $(A_t - A_\infty) = (A_0 - A_\infty)\exp(-k_{obsd}t)$ (for 530 and 474 nm, A_t values were taken after 8–10 half-lives of the rapid phase had elapsed). The resulting values of k_{obsd}^{474} or k_{obsd}^{530} and k_{obsd}^{iso} were fitted to eq 2 and 3, respectively, to obtain values of a, b, c, and d. At 474 nm, $a = 1.05 \times 10^3$ M^{-1} s^{-1} and $b = 2.57 \times 10^2$ M^{-1}. At 530 nm, $a = 1.03 \times 10^3$ M^{-1} s^{-1} and $b = 2.65 \times 10^2$ M^{-1} s^{-1}. At the isosbestic wavelengths, $c = 14.5$ s^{-1} and $d = 3.73 \times 10^3$ M^{-1} s^{-1}. Now we consider the significance of the k_{obsd}^{474} or k_{obsd}^{530} and k_{obsd}^{iso} on the basis of Scheme I. The measurements of the rapid phase at the isobestic wavelength are expected to be a measure of all pathways for the disappearance of $[Ru(NH_3)_5(pz)]^{3+}$ and its equilibration with I, and therefore $k_{obsd}^{iso} = k_{-1} + (k_1 + k_2)[[Co(EDTA)]^{2-}]$. The measurements of the slow phase at 530 or 474 are given by the expression k_{obsd}^{530} or $k_{obsd}^{474} = k_2[[Co(EDTA)]^{2-}]/(1 + (k_1/k_{-1})[[Co(EDTA)]^{2-}])$ *if* the rapid phase has reached equilibrium before the onset of the slow phase. It will be seen that according to the above interpretation and the input parameters, $k_{obsd}^{iso} = 15 + (4 \times 10^3)$-$[[Co(EDTA)]^{2-}]$ and k_{obsd}^{474} or $k_{obsd}^{530} = 1 \times 10^3/(1 + 200$-$[[Co(EDTA)]^{2-}])$, to be compared with the results of the kinetic modeling $k_{obsd}^{iso} = 14.5 + (3.73 \times 10^3)[[Co(EDTA)]^{2-}]$, $k_{obsd}^{474} = 1.05 \times 10^3/(1 + (2.57 \times 10^2)[[Co(EDTA)]^{2-}])$, and $k_{obsd}^{530} = 1.03 \times 10^3/(1 + (2.65 \times 10^2)[[Co(EDTA)]^{2-}])$. Evidently, within 6% accuracy, a, c, and d can be identified with k_2, k_{-1}, and $k_1 + k_2$, respectively. However, b (2.6×10^2) is somewhat larger than k_1/k_{-1} (2×10^2) and almost equal to d/c (257), which is identified as $(k_1 + k_2)/k_{-1}$. It is apparent that the interpretation offered above of the significance of k_{obsd}^{iso} and k_{obsd}^{474} or k_{obsd}^{530} represents an acceptable approximation to estimate the constants in Scheme I, except perhaps k_1/k_{-1}.[17] The later value can be estimated as $(d - a)/c$.

The measurements of the slow phase conform to the equations $k_{obsd}^{474} = 8.8 \times 10^2/(1 + (4.2 \times 10^2)[(Co(EDTA))^{2-}])$ and $k_{obsd}^{530} = 1.1 \times 10^3/(1 + (4.6 \times 10^2)[(Co(EDTA))^{2-}])$, respectively. Therefore, $k_2 = (1.0 \pm 0.1) \times 10^3$ M^{-1} s^{-1} and $k_1/k_{-1} = (4.4 \pm 0.2) \times 10^2$ M^{-1}. The measurements of the rapid phase conform to $k_{obsd}^{iso} = 16.9 + (3.53 \times 10^3)[(Co(EDTA))^{2-}]$. Therefore, $k_1 + k_2 = 3.5 \times 10^3$ M^{-1} s^{-1} and $k_{-1} = 16.9$ s^{-1}. Finally, the measurements of the reverse reaction conform to the equation $k_{obsd}^{384} = 3.5 \times 10^{-5} + 3.2[(Ru(NH_3)_5(pz))^{2+}]$. Therefore, the rate constant for direct reduction of $[Co(EDTA)]^-$ by ascorbic acid is $\sim 2 \times 10^{-2}$ M^{-1} s^{-1} and $k_{-2} = 3.2$ M^{-1} s^{-1}. It will be seen that the experimental results conform reasonably well to those of the kinetic modeling with two exceptions. First, the kinetic modeling shows that the rate constants for the slow phase should be wavelength independent, whereas we observe that the values of k_{obsd}^{474} (and the derived value of k_1) are $\sim$15–20% smaller than the values of k_{obsd}^{530}. Second, the kinetic modeling shows that k_1/k_{-1} derived from k_{obsd}^{474} or k_{obsd}^{530} and $(k_1 + k_2)/k_{-1}$ derived from k_{obsd}^{iso} are almost equal, whereas the experimental results show a discrepancy of almost a factor of 2.2 between these two quantities. We do not have an entirely satisfactory explanation for the discrepancies, but kinetic complications in systems of this type have been observed previously[7,18] and have been ascribed to

(15) Since the 474-nm band of $[Ru(NH_3)_5(pz)]^{2+}$ is a metal to ligand charge-transfer band, addition of electropositive substituents to the remote N of pyrazine is expected to produce a bathochromic shift in the MLCT band. See, for example: Jwo, J. J.; Gaus, P. L.; Haim, A. *J. Am. Chem. Soc.* **1979**, *101*, 6189.

(16) Calculations were performed on a Digital Equipment Corporation 11V03 computer using the program RLINKLIT: Johnson, K. J. "Numerical Methods in Chemistry"; Marcel Dekker: New York, 1980; p 351.

(17) An exact treatment of the data does not seem feasible at the present time. Neglecting the back reaction k_{-2} (a good approximation since the equilibrium in eq 1 is more than 99% complete at all concentrations of $[Co(EDTA)]^{2-}$), the differential equations derived from Scheme I can be integrated. However, not enough points were collected during the initial rapid phases at 530 and 474 nm.

(18) Isied, S. S.; Taube, H. *J. Am. Chem. Soc.* **1973**, *28*, 8198.

Scheme II

$$[Ru(NH_3)_5(pz)]^{3+} + [Co(EDTA)]^{2-} \underset{k_{-1}}{\overset{k_1}{\rightleftharpoons}} [(NH_3)_5Ru^{II}(pz)Co^{III}(EDTA)]^{+}$$

$$k_3 \Big\downarrow \Big\uparrow k_{-3}$$

$$[Ru(NH_3)_5(pz)]^{2+} + [Co(EDTA)]^{-}$$

oxidation of the binuclear complexes $[(NC)_5Fe^{II}(CN)Co^{III}(EDTA)]^{5-}$ or $[(H_2O)(NH_3)_5Ru^{II}NC_5H_4\text{-}4\text{-}CO_2Co^{III}(NH_3)_5]^{4+}$ by $[Fe(CN)_6]^{3-}$ or $[Ru(NH_3)_4(OH_2NC_5H_4\text{-}4\text{-}CO_2]^{2+}$. Similarly, we postulate the oxidation of I by $[Ru(NH_3)_5(pz)]^{3+}$, eq 6.

$$[(NH_3)_5Ru^{II}(pz)Co^{III}(EDTA)]^{+} + [Ru(NH_3)_5(pz)]^{3+} \rightleftharpoons [(NH_3)_5Ru^{III}(pz)Co^{III}(EDTA)]^{2+} + [Ru(NH_3)_5(pz)]^{2+} \quad (6)$$

Adding eq 6 to Scheme I accounts for some of the discrepancies noted above.[19]

On the basis of the above considerations, we believe the values of k_2 (1.0×10^3 M^{-1} s^{-1}), $k_1 + k_2$ (3.5×10^3 M^{-1} s^{-1}), k_{-1} (16.9 s^{-1}), k_1/k_{-1} ($(3.5 \times 10^3 - 1.0 \times 10^3)/16.9 = 148$ M^{-1}), and k_{-2} (3.2 M^{-1} s^{-1}) to be rather good approximations of the true values. An independent estimate of the value of k_2 can be obtained by combining the measured value of k_{-2} (3.2 M^{-1} s^{-1}) with the value of the equilibrium constant K_2 ($\equiv k_2/k_{-2}$) calculated from the reduction potentials of the ruthenium[12,13] and cobalt[14] couples. With $K_2 = 343$, we obtain $k_2 = 1.1 \times 10^3$ M^{-1} s^{-1}, in remarkable agreement with k_2 derived from the measurements of the slow phase. Additional confirmation of the value of k_2 comes from calculations using the Marcus cross relationship (ion-pair approach[20]). With rate constants for self-exchange 4.5×10^5 M^{-1} s^{-1} and 3.5×10^{-7} M^{-1} s^{-1} and radii 3.5×10^{-8} and 4.0×10^{-8} cm for the ruthenium[21] and cobalt[8] couples, respectively, the calculated value of k_2 is 5.9×10^2 M^{-1} s^{-1}, in excellent agreement with the measured value.

So far, back electron transfer in I followed by outer-sphere reaction between $[Ru(NH_3)_5(pz)]^{3+}$ and $[Co(EDTA)]^{2-}$ has been taken to be the only route from I to the final products $[Ru(NH_3)_5(pz)]^{2+}$ and $[Co(EDTA)]^{-}$. An alternative or additional route involves direct dissociation of I to $[Ru(NH_3)_5(pz)]^{2+}$ and $[Co(EDTA)]^{-}$ (Scheme II). The mechanistic patterns embodied in Schemes I and II were considered previously[5,8] for the $[Fe(CN)_6]^{3-}$–$[Co(EDTA)]^{2-}$ and $[Fe(CN)_5L]^{2-}$ (L = pyridine or 4,4′-bipyridine)–$[Co(EDTA)]^{2-}$ systems. With the information available for the iron systems, Schemes I and II are kinetically indistinguishable. However, from the indirect arguments based on comparisons of substitution rates of Co^{III}–EDTA complexes, it was argued[5,8] convincingly[22,23] that Scheme II is not operative; i.e., the successor binuclear complex I represents a dead end. Similar indirect arguments can be advanced for the present system.[24] However, it is not necessary to do so: *the data obtained give direct proof that Scheme I provides the bulk of the reaction pathway*, with Scheme II providing at the most a minor contribution. The information necessary to determine the relative contributions of Scheme I and II is contained in the absorbance vs. time data at 474 or 530 nm. The calculations are not very sensitive at 530 nm, and therefore only the 474-nm data was processed. By integration of the mechanism represented by Schemes I and II, it can be shown that the absorbance of the slow phase extrapolated to time zero is given by eq 7, where a_{Ru} is the

$$A_0^{474} = \frac{a_B T' + a_{Ru} T'(L_2 - 1)}{(L_2 - L_1)M_1} \quad (7)$$

molar absorbance of $[Ru(NH_3)_5(pz)]^{2+}$, $T' = (k_1 + k_2 - L_1k_1)[(Ru(NH_3)_5(pz))^{3+}]_0$, $L_1 = k_{-1}/(k_{-1} + k_3 - M_1)$, $L_2 = k_{-1}/(k_{-1} + k_3 - M_2)$, $M_{1,2} = [(k_1 + k_2 + k_{-1} + k_3)/2] \pm [0.25(k_1 + k_2 - k_{-1} - k_3)^2 + k_1k_{-1}]^{1/2}$. It will be seen that the value of A_0^{474} is sensitive to the mechanism. If only Scheme II is operative, only I contributes to A_0^{474}. If Scheme I is also operative, then A_0^{474} will be larger because of the contribution to A_0^{474} of the $[Ru(NH_3)_5(pz)]^{2+}$ produced in the rapid phase. Experimental values of A_0^{474} are listed in column 2 of Table III. In columns 3 and 4 we list values of A_0^{474} calculated under the assumption that *either* Scheme I or Scheme II is operative.[25] It will be seen that, except for the lowest concentration of $[Co(EDTA)]^{2-}$, the agreement between columns 2 and 3 is excellent, and we conclude that Scheme I constitutes the major reaction pathway and estimate that Scheme II contributes less than 10% to the overall reaction.

It is instructive to compare the relative outer- and inner-sphere reactivities of $[Ru(NH_3)_5(pz)]^{3+}$ and $[Ru(NH_3)_5(bpy)]^{3+}$ vs. $[Co(EDTA)]^{2-}$. The experimental ratio of the outer-sphere rate constants k_{pz}^{os}/k_{bpy}^{os} is 13, in good agreement with the value 33 calculated from the square root of the difference in reduction potentials between $[Ru(NH_3)_5(pz)]^{3+}$ (0.52 V) and $[Ru(NH_3)_5(bpy)]^{3+}$ (0.34 V) expressed as an equilibrium constant. The agreement between the experimental value of the ratio and the value calculated on the basis of the thermodynamic barrier only implies that the rate constants for self-exchange in the $[Ru(NH_3)_5(pz)]^{3+/2+}$ and $[Ru(NH_3)_5(bpy)]^{3+/2+}$ systems are substantially the same, as observed for other complexes of pentaammineruthenium with pyridine derivatives.[21] With regard to the inner-sphere reactivity k_{pz}^{is}/k_{bpy}^{is}, it is noteworthy that the inner-sphere pathway was not detected in the $[Ru(NH_3)_5(bpy)]^{3+}$–$[Co(EDTA)]^{2-}$ system[8] whereas a rate constant of 2.5 $\times 10^3$ M^{-1} s^{-1} is found in the corresponding pyrazine system. Assuming that the reactivity differences between the pyrazine and

Table III. Comparison of Experimental and Calculated Values of A_0^{474} [a]

10^3-[[Co(EDTA)]$^{2-}$], M	$10^2A_0^{474}$ [b]	$10^2A_0^{474}$ [c]	$10^2A_0^{474}$ [d]
1.22	2.1, 1.8	0.94	0.41
2.45	1.7, 1.9, 2.1, 2.2	1.84	0.84
3.67	2.4, 2.9, 3.0	2.60	1.23
4.84	3.1, 3.2, 3.9	3.20	1.56
6.29	3.2, 3.6	3.80	1.92
7.25	4.0, 4.4	4.12	2.13

[a] All values normalized to $[Ru(NH_3)_5pz^{3+}]_0 = 1.0 \times 10^{-5}$ M, 1-cm path length. [b] Obtained by extrapolation to zero time of the A_t^{474} vs. time plots. [c] Calculated from eq 6 on the basis of Scheme I with $k_1 = 2.5 \times 10^3$ M^{-1} s^{-1}, $k_2 = 1.0 \times 10^3$ M^{-1} s^{-1}, $k_{-1} = 16.9$ s^{-1}. [d] Calculated from eq 6 on the basis of Scheme II with $k_1 = 3.5 \times 10^3$ M^{-1} s^{-1}, $k_{-1} = 16.9$ s^{-1}, $k_3 = 4.8$ s^{-1}.

(19) A kinetic modeling as described above but incorporating eq 6 to Scheme I yields the following values (input values in Scheme I are the same as above; rate constants for the forward and reverse reactions in eq 6 are taken as 1×10^5 M^{-1} s^{-1}, the self-exchange rate constant for $[Ru(NH_3)_5L]^{3+/2+}$ complexes where L is a pyridine derivative): k_2(474 nm) = 1.2×10^3 M^{-1} s^{-1}; k_1/k_{-1}(474 nm) = 304 M^{-1}; k_2(530 nm) = 1.7×10^3 M^{-1} s^{-1}; k_1/k_{-1}(530 nm) = 429 M^{-1}; k_{-1}(isosbestic) = 15.3 s^{-1}; $k_1 + k_2$(isosbestic) = 3.67×10^3 M^{-1} s^{-1}.

(20) Oliveira, L. A. A.; Haim, A. *J. Am. Chem. Soc.* **1982**, *104*, 3363.

(21) Brown, G. M.; Krentzien, H. J.; Abe, M.; Taube, H. *Inorg. Chem.* **1979**, *18*, 3374.

(22) Taube, H. *Pure Appl. Chem.* **1975**, *44*, 25.

(23) Reagor, B. T.; Huchital, D. H. *Inorg. Chem.* **1982**, *21*, 703.

(24) On the basis of Scheme II and the measured constants, k_3 is calculated to be a $c/(d - a) = 6.7$ s^{-1} and represents the loss of $[Ru(NH_3)_5(pz)]^{2+}$ from the coordination sphere of a pentadentate Co(III)–EDTA complex. Similar reactions, such as loss of Cl^- from $[Co(EDTA)Cl]^{2-}$, occur with rate constants $\sim 10^{-6}$ s^{-1}. Therefore, $k_3 = 6.7$ s^{-1} is considered an unreasonably high rate for a substitution reactions at the Co^{III}(EDTA) center.

(25) The data from the kinetic modeling of Scheme I were also treated, and it was found that the values of A_0^{474} obtained by extrapolation to $t = 0$ of the A_t^{474} data are ($[Co(EDTA)]^{2-}$ concentration in parentheses) 0.0101 (1.0×10^{-3}), 0.0189 (2.0×10^{-3}), 0.0317 (4.0×10^{-3}), and 0.0438 (7.0×10^{-3}). Values calculated from eq 6 are 0.0101, 0.0191, 0.0324, and 0.0441. A kinetic modeling of Scheme II was also carried out with $k_1 = 3 \times 10^3$ M^{-1} s^{-1}, $k_{-1} = 15$ s^{-1}, and $k_3 = 5$ s^{-1}. Values of A_0^{474} obtained by extrapolation are 0.00268 (1×10^{-3}), 0.00555 (2×10^{-3}), 0.0112 (4×10^{-3}), and 0.0196 (7×10^{-3}). Values calculated from eq 6 are 0.00258, 0.00554, 0.0114, and 0.0197. The calculations show that the comparison between extrapolated values of A_0^{474} and calculated values on the basis of either Scheme I or Scheme II serves to make a distinction between the two mechanisms.

bipyridine complexes arise solely from thermodynamic differences, the ratio k_{pz}^{is}/k_{bpy}^{is} should be 33, the same value as for the corresponding outer-sphere reaction. However, the distance between the metal centers is presumably different for inner-sphere and outer-sphere transition states. Calculations[8] suggest that outer-sphere electron transfer corresponds to a distance of closest approach between metal centers of 7×10^{-8} cm in $[Ru(NH_3)_5L]^{3+}$–$[Co(EDTA)]^{2-}$, independent of the nature of L when L = pyridine or 4,4′-bipyridine. In contrast, the metal to metal distances are very different in the $[(NH_3)_5Ru(pz)Co(EDTA)]^+$ (6.9×10^{-8} cm) and $[(NH_3)_5Ru(bpy)Co(EDTA)]^+$ (11.1×10^{-8} cm) inner-sphere transition states. In previous work[2] we found that the distance dependence of rate constants for intramolecular electron transfer in $[(NC)_5Fe(L)Co(NH_3)_5]$ and $[(EDTA)Ru(L)Co(NH_3)_5]^+$ (L = pyrazine or a bipyridine) is given by eq 8,

$$\lambda_0 = e^2\left(\frac{1}{2a_1} + \frac{1}{2a_2} - \frac{1}{r}\right)\left(\frac{1}{D_{op}} - \frac{1}{D_s}\right) \qquad (8)$$

the outer-sphere reorganization energy,[26] where a_1 and a_2 are the radii of the two reactants, r is the distance between the metal centers in the transition state, and D_{op} and D_s are the optical and static dielectric constant of the medium, respectively. On the basis of eq 8, the expected ratio of inner-sphere reactivities for pyrazine and 4,4′-bipyridine is 65 (to be compared with experimental values of 21 and 30 for $[(NC)_5Fe(L)Co(NH_3)_5]$[27] and $[(EDTA)Ru(L)Co(NH_3)_5]^+$[28], respectively). On the basis of the thermodynamic barrier and the distance effect, the calculated value of k_{pz}^{is}/k_{bpy}^{is} is 33×65 or 2.1×10^3 and $k_{bpy}^{is} = 2.5 \times 10^3/(2.1 \times 10^3) = 1.2\ M^{-1}\ s^{-1}$. Evidently, such small contribution of the inner-sphere path to the overall $[Ru(NH_3)_5(bpy)]^{3+}$–$[Co(EDTA)]^{2-}$ reaction ($k_{bpy}^{os} = 77\ M^{-1}\ s^{-1}$) could not have been detected.[8]

Finally, it is of interest to compare the value of the rate constant $16.9\ s^{-1}$ for intramolecular electron transfer in $[(NH_3)_5Ru^{II}(pz)Co^{III}(EDTA)]^+$ measured in the present work with the value $8 \times 10^9\ s^{-1}$ reported previously[12] for intramolecular electron transfer in the very similar system $[(NH_3)_5Ru^{II}(pz)Ru^{III}(EDTA)]^+$. Since the thermodynamic factors are probably not very different for the Ru^{II}/Co^{III} and Ru^{II}/Ru^{III} systems,[29] the difference in intramolecular electron-transfer rates reflects mostly the difference in rate constants for self-exchange in $[Ru(EDTA)]^{2-/-}$ vs. $[Co(EDTA)]^{2-/-}$. Undoubtedly,[30] a major portion of the difference in the rate constants for exchange is associated with the much smaller inner-sphere configuration changes in $[Ru(EDTA)^{-/2-}$ as compared to $[Co(EDTA)]^{-/2-}$. Whether orbital symmetry considerations are also important in determining the difference in the rates of exchange remains to be seen.[31]

Registry No. I, 88440-69-1; $[Ru(NH_3)_5(pz)]^{3+}$, 38139-16-1; $[Co(EDTA)]^{2-}$, 14931-83-0.

(26) Callahan, R. W.; Keene, F. R.; Meyer, T. J.; Salmon, D. J. *J. Am. Chem. Soc.* **1977**, *99*, 1064.
(27) Szecsy, A. P.; Haim, A. *J. Am. Chem. Soc.* **1981**, *103*, 1679.
(28) Oliveira, L. A. A. de; Haim, A. "Abstracts of Papers", 183rd Meeting of the American Chemical Society, Las Vegas, 1982; American Chemical Society: Washington, D.C., 1982; INOR 235.
(29) $E°$ for $(NH_3)_5Ru^{III}(pz)Ru^{III}EDTA^+ + e^- \rightarrow (NH_3)_5Ru^{III}(pz)Ru^{II}EDTA$ has been estimated as 0.37 V,[12] identical with the $E°$ for $CoEDTA^{-/2-}$.
(30) Sutin, N. *Prog. Inorg. Chem.* **1983**, *30*, 441.
(31) Brunschwig, B. S.; Creutz, C.; Macartney, D. H.; Sham, T.-K.; Sutin, N. *Faraday Discuss. Chem. Soc.* **1982**, *74*, 113.

Reactivity of 2-(Diphenylphosphino)pyridine toward Complexes Containing the Quadruply Bonded Re_2^{6+} Core: Ortho Metalation and Redox Chemistry

Timothy J. Barder,[1a] F. Albert Cotton,*[1b] Gregory L. Powell,[1b] Stephen M. Tetrick,[1a] and Richard A. Walton*[1a]

Contribution from the Department of Chemistry, Purdue University, West Lafayette, Indiana 47907, and the Department of Chemistry and Laboratory for Molecular Structure and Bonding, Texas A&M University, College Station, Texas 77843. *Received July 28, 1983*

Abstract: The quadruply bonded dirhenium(III) complexes $(n\text{-}Bu_4N)_2Re_2Cl_8$ and $Re_2Cl_6(PR_3)_2$ (R = Et or *n*-Bu) react in methanol with 2-(diphenylphosphino)pyridine (Ph_2Ppy) to afford complexes that are derivatives of the triply bonded dirhenium(II) core, Re_2^{4+}. The complex $Re_2Cl_4(Ph_2Ppy)_3$ (I) is formed initially and is found to eliminate HCl to give the ortho-metalated complex $Re_2Cl_3(Ph_2Ppy)_2[(C_6H_5)(C_6H_4)Ppy]$ (II), the first example of a reaction of this type occurring at a metal–metal multiple bond of the M_2L_8 type. Both chloride and hexafluorophosphate salts of the $[Re_2Cl_2(Ph_2Ppy)_4]^{2+}$ dication (III) have been isolated (Cl^-, IIIa; PF_6^-, IIIb); III constitutes a rare example of a multiply bonded dimetal unit complexed by four neutral bridging ligands. $[Re_2Cl_2(Ph_2Ppy)_4]Cl_2$ can be converted to either I or II under certain conditions. When acetone is used as the solvent, then $Re_2Cl_6(PR_3)_2$ reacts with Ph_2Ppy to give $Re_2Cl_4(Ph_2Ppy)_2(PR_3)$ (R = Et, IVa; R = *n*-Bu, IVb), whereas with acetonitrile as the solvent, Ph_2Ppy converts $(n\text{-}Bu_4N)_2Re_2Cl_8$ to the dirhenium(III) complex $Re_2(\mu\text{-}Cl)_2(\mu\text{-}Ph_2Ppy)_2Cl_4$; i.e., substitution occurs but without concomitant reduction. The complexes II, IIIb, and IVa have been structurally characterized by X-ray crystallography. Compound II crystallizes in space group $P2_1/n$ with $a = 12.160$ (6) Å, $b = 21.418$ (7) Å, $c = 18.464$ (2) Å, $\beta = 99.04$ (3)°, and $Z = 4$. Complex IIIb forms crystals in space group $P2_1/c$ with $a = 24.316$ (3) Å, $b = 12.101$ (2) Å, $c = 27.070$ (3) Å, $\beta = 105.670$ (9)°, and $Z = 4$. Two acetone molecules per dimer unit are also present in the lattice. Compound IVa crystallizes in space group $P\bar{1}$ with $a = 10.683$ (2) Å, $b = 20.033$ (5) Å, $c = 10.544$ (3) Å, $\alpha = 102.29$ (3)°, $\beta = 107.69$ (2)°, $\gamma = 94.19$ (2)°, and $Z = 2$.

Monodentate tertiary phosphines form a variety of well-defined complexes with the halides of Nb, Ta, Mo, W, and Re that contain dimetal units with metal–metal bonds of order two (Nb and Ta), three (Re), or four (Mo, W, and Re).[2] In the case of Nb and Ta, these complexes are chlorine-bridged molecules of stoichiometry $M_2X_6(PR_3)_4$, whereas the Mo, W, or Re species are either $Re_2X_6(PR_3)_2$ or $M_2X_4(PR_3)_4$ (M = Mo, W, or Re) and possess eclipsed M_2L_8-type rotational geometries.[2] However, with

(1) (a) Purdue University. (b) Texas A & M University.
(2) Cotton, F. A.; Walton, R. A. "Multiple Bonds between Metal Atoms"; Wiley: New York, 1982 and references therein.

0002-7863/84/1506-1323$01.50/0